Reply on RC1

This is a well-conceptualised and thoroughly documented study that adds to our knowledge of the occurrence of loess funnels on the Chinese Loess Plateau. The authors conducted field research using UAVs (photogrammetry and aerial laser scanning) and handheld laser scanning to inventory and quantitatively estimate the occurrence of loess sinkholes in a typical loess catchment. The authors proposed indicators and methods for the morphological quantification of loess sinkholes and compiled a dataset containing 1,194 records at the catchment scale. They analyzed the spatial distribution of loess sinkholes in the catchment area and identified spatial patterns, performed a morphological analysis, and analyzed the fit of morphometric parameters. They also estimated subsurface soil erosion and quantified the impact of various factors on the formation of loess sinkholes. The article thus provides a better understanding of the causes and mechanisms of loess sinkhole formation. The structure of the manuscript is correct, the concept and purpose of the study are clearly defined, and the methodology is correctly selected and well described. The results and discussion introduce new knowledge, and the conclusions accurately reflect the achievements of this study.

Reply: We are deeply grateful for your recognition of our research on loess sinkholes on the Chinese Loess Plateau, which makes us feel extremely honored and proud. Your positive comments have given us confidence to continue conducting research at larger scales and deeper levels in the future. Meanwhile, we will also carefully revise and improve the manuscript according to the comments from other reviewers and editors. Thank you once again for the time you have spent reviewing this paper with great patience, as well as your fair and well-intentioned suggestions!

Reply on RC2

General comments

The paper describes a comprehensive survey of sinkholes in a catchment of the Chinese Loess Plateau using UAV- and handheld LiDAR-based remote sensing. The authors report statistics on sinkhole characteristics and examine spatial statistical relationships between topographic and geomorphological factors on the one hand, and the occurrence of sinkholes on the other. The three-dimensional measurement of sinkhole volumes allows for much more accurate estimates of soil loss than simplified geometric methods. The research objective is clearly defined, the methodology is appropriate, and the results are reproducible. The figures are generally informative and well-designed, aside from minor errors (see below). Results and discussion expand the knowledge of sinkholes in loess deposits, and open sharing of the collected field data allows for scientific reuse. The submitted data is complete and supplied in accessible formats.

Reply: First of all, on behalf of all the authors, I would like to express my sincere gratitude for your diligent review and thank you very much for your recognition of our research. Your General Comments are greatly encouraging to us, although the manuscript still has much room for improvement at this stage. Next, we will revise and refine the paper according to your Specific Comments.

Specific comments

The percentages reported in the "Results" section do not seem to add up. Most are correctly calculated based on a denominator of 1,194, while others appear to refer to a denominator of approximately 809. I have listed a few examples below, but I recommend that all values be carefully checked again.

Reply: Thank you very much for your careful observation! Let me explain why the total sample count of elevation is 809 rather than 1194: First, we indeed interpreted 1194 sinkholes from the UAV imagery, as the high-resolution images do allow us to

identify smaller features (such as those with diameters less than 1 m). However, since the UAV flight altitude was around 200 m, the point cloud density from the airborne LiDAR was not particularly high. Our inspection revealed that the LiDAR point clouds were very sparse when detecting sinkholes with diameters below 1 m, with some sinkholes having only a few points, making it difficult to accurately capture parameters related to depth and volume. Therefore, when calculating maximum elevation, maximum depth, volume, and length to depth ratio, we only included sinkholes with diameters greater than 1 m. In fact, we have already indicated the sample sizes in Figure 9. To avoid any confusion, we feel it is necessary to provide a brief explanation in the main text of Section 4.3 Morphometric analysis. We have carefully checked all values again. Thank you once again for your thoughtful comment!

4.3 Morphometric analysis

Here below we analyze the spatial and morphometric parameters computed for the 1194 inventoried sinkholes (1162 single, 32 compound), their frequency-size distribution (Fig. 9), as well as some spatial patterns based on the distribution of different value ranges (Fig. 10). It should be noted that the airborne LiDAR returned sparse and limited point clouds when detecting sinkholes with diameters less than 1 m. When calculating parameters related to sinkhole depth and volume (e.g., Maximum Elevation, Maximum Depth, Volume, and Length-to-Depth Ratio), we retained only 809 sinkholes with diameters $\geqslant$1 m.

G	H	I	J	K	L	M	N	O	P	Q	R	S	T	U
方位角1	方位角2	最大高程	最小高程	平均高程	最大深度	周长	面积	体积	延伸率	直径/深度比	紧实度指数	圆度指数	土壤干密度	土壤流失量
Azimuth 1	Azimuth 2	Maximum elevation	Minimum elevati	Average elevatio	Maximum depth	Perimeter	Area	Volume	Elongation ratio	Length to Depth ratio	Compactness index	Circularity index	Soil dry density	Soil loss
Azi_1	Azi_2	Emax	Emin	Eave	Dmax	P	A	V	ER	LDr	COI	CLI	ρ_dry	SL
°	°	m	m	m	m	m	m^2	m^3	-	-	-	-	t/m^3	t
177.9	357.9	2016.66	2012.52	2014.50	4.14	14.52	15.44	63.89	1.48	1.28	0.81	0.92	1.274	81.39
10.0	190.0					2.74	0.57		1.17		0.77	0.95	1.274	
127.9	307.9					1.95	0.27		1.36		0.69	0.89	1.274	
24.6	204.6					2.58	0.40		1.36		0.69	0.76	1.274	
108.4	288.4	1987.40	1979.14	1984.46	8.26	15.61	18.78	155.15	1.11	0.63	0.76	0.97	1.274	197.66
21.8	201.8	1986.14	1979.61	1983.79	6.53	16.25	18.99	124.06	1.12	0.77	0.85	0.90	1.274	158.05
92.9	272.9	1985.51	1979.75	1982.47	5.76	18.79	26.00	149.68	1.38	1.18	0.77	0.93	1.274	190.70
41.6	221.6	1994.71	1991.88	1993.31	2.83	4.34	1.23	3.47	1.76	0.57	0.82	0.82	1.274	4.42
96.6	276.6	1995.06	1987.58	1992.65	7.48	6.42	3.15	23.54	1.05	0.27	0.80	0.96	1.274	29.99
125.4	305.4	2014.31	2009.89	2012.53	4.42	5.79	2.42	10.70	1.44	0.48	0.78	0.91	1.274	13.64
165.5	345.5	2013.60	2008.16	2011.10	5.44	7.04	3.61	19.62	1.14	0.42	0.80	0.91	1.274	25.00
114.4	294.4					2.80	0.58		1.40		0.79	0.93	1.274	
94.5	274.5					2.62	0.51		1.26		0.73	0.93	1.274	
137.8	317.8					2.36	0.39		1.47		0.76	0.87	1.274	
19.7	199.7					3.57	0.85		1.54		0.76	0.83	1.274	
76.9	256.9	1992.94	1991.58	1992.01	1.37	6.62	2.87	3.91	1.62	1.84	0.73	0.82	1.274	4.99
50.6	230.6	1992.82	1991.96	1992.33	0.85	4.00	1.18	1.01	1.40	1.68	0.81	0.93	1.274	1.28
149.5	329.5	1920.51	1919.01	1920.21	1.50	4.01	1.07	1.62	1.86	1.06	0.78	0.84	1.274	2.06
161.1	341.1	1920.52	1919.18	1920.17	1.34	4.00	1.10	1.47	1.63	1.14	0.77	0.86	1.274	1.88
19.2	199.2	1922.84	1918.25	1919.64	4.58	8.24	5.03	23.07	1.37	0.65	0.78	0.93	1.274	29.39
17.0	197.0	1958.50	1956.42	1957.73	2.09	10.39	3.64	7.60	1.95	1.84	0.48	0.42	1.274	9.68
42.7	222.7	1907.81	1904.86	1907.03	2.95	4.30	1.25	3.68	1.60	0.56	0.73	0.85	1.274	4.69
3.0	183.0					3.23	0.78		1.34		0.83	0.93	1.274	
159.4	339.4	1909.05	1907.21	1908.11	1.84	7.73	4.22	7.75	1.20	1.38	0.79	0.89	1.274	9.87
11.6	191.6					3.40	0.71		1.74		0.71	0.77	1.274	
2.3	182.3	1908.82	1908.24	1908.57	0.58	4.68	1.08	0.63	1.53	2.66	0.70	0.62	1.274	0.80
42.9	222.9	1908.93	1907.99	1908.44	0.94	9.94	5.97	5.63	1.36	3.70	0.67	0.76	1.274	7.17
6.3	186.3	1908.91	1906.97	1908.20	1.93	6.86	2.73	5.27	2.19	1.45	0.76	0.73	1.274	6.71
63.7	243.7	1862.44	1844.33	1852.14	18.11	57.75	236.27	4278.30	1.19	1.06	0.76	0.89	1.274	5450.55

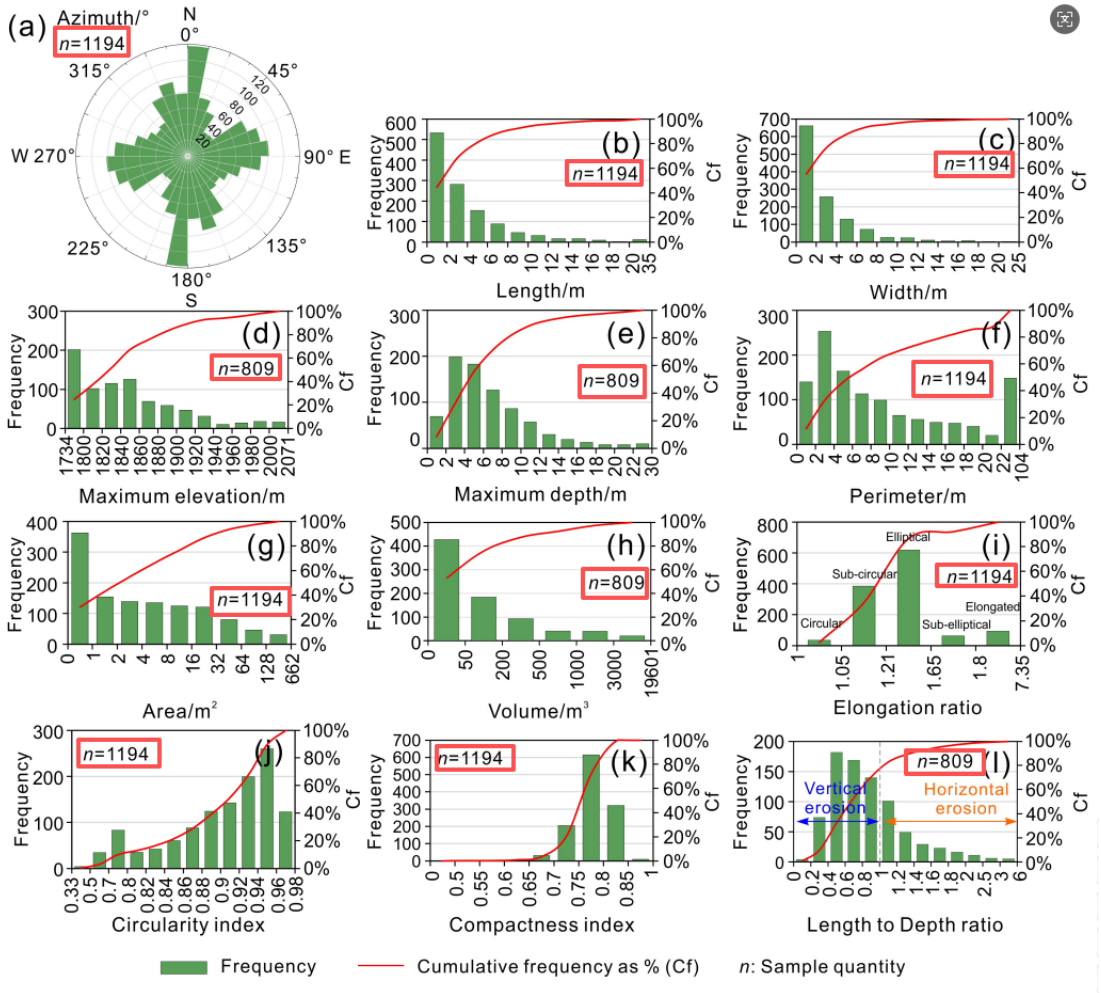

l 520f: The authors state that the piping developed at a former footslope position, which implies it formed on the elevation of the then-active main channel. Subsequently, the channel incised as a result of uplift, such that the sinkhole is now situated at an elevation of approximately 8 m above the present channel level. I am surprised, however, that the massive landslide on the opposite slope is not considered in this interpretation. As illustrated in Fig. 14a, the toe of the landslide is being undercut, indicating that the river continues to erode its deposits. Progressive reworking of the landslide-derived valley fill, and the associated temporary damming of the channel, could also account for the backflood deposits within the pipe (l. 535) as well as the stratified flood deposits observed on the fluvial terrace (l. 529). This implies a much younger age of the piping and sinkhole formation than the one suggested by valley incision.

Reply: Thank you for this very insightful comment. Due to the lack of accurate chronological evidence, we indeed cannot confirm at present whether this particular

sinkhole formed prior to river incision. Therefore, I feel that our previous inference may not have been sufficiently rigorous. Upon reviewing the field photos we took, I found that the giant landslide on the opposite bank of this sinkhole did completely block the river channel at that time, which could have led to landslide or dammed-lake sediments entering this sinkhole. I fully agree with your interpretation. We have revised this part of the discussion accordingly.

Interestingly, most sinkholes examined in the field display dominant vertical development, while this particular sinkhole exhibits a complex three-dimensional morphology comprising a vertical shaft connected to a subhorizontal pipe. The upper shaft-like portion of the sinkhole (20 m length × 14 m width × 20.1 m depth) is situated in loess deposits, while the lower portion (14 m length × 3.2 m width × 5.4 m height) is a gently inclined ellipsoidal conduit carved into horizontally bedded and jointed reddish sandstone. This lower conduit ends at the sinkhole outlet perched 8 m above the valley floor (Fig. 14a). However, it is regrettable that due to the lack of precise chronological evidence, we are unable to determine whether the initial development of this sinkhole predates or postdates the valley incision. We interpret that the development of this complex sinkhole started as a backward propagating conduit at the foot of the slope, associated with a seepage outlet point controlled by joints in the loess cover and the bedrock (Figs. 14d-h). Eventually, the enlarging conduit reached a sufficiently large span to initiate upward roof collapse, ultimately originating the sinkhole. At present, five distinct ceiling cupolas can be clearly observed at the top of this pipe (Figs. 14b, c and i), indicating sites of upward roof propagation (stoping).

Additionally, we observed a significant accumulation of horizontally stratified flood deposits resting atop the aeolian loess on the fluvial strath terrace (Fig. 14a). The interior of the sinkhole is relatively cool and damp, with the bottom underlain by collapsed soil. We found remnants of past flash-flood or debris-flow deposits on the sinkhole floor, as well as on the walls and outlet ceiling of the connected lateral pipe (Figs. 14d, f, j). These sediments may include: (1) Horizontally bedded deposits

accumulated during floods in the drainage, with a stage high enough to cause the penetration of flood waters into the sinkhole outlet (backflooding); (2) Massive to poorly stratified deposits derived from collapse and mass wasting processes acting primarily in the pipe roof and sinkholes margins, respectively. It should be particularly noted that the largest loess landslide in this basin occurred on the opposite bank of this sinkhole. Based on field investigations, we believe that this landslide completely blocked the paleo-channel at that time, forming a small-scale dammed lake, and the landslide deposits and lacustrine sediments could easily enter the interior of the sinkhole through lateral pipe.

l 589–622: The authors describe covincingly the influence of gullies and landslides on sink holes and piping. I suggest adding, that this relationship is not unidirectional, but the results of interconnected processes and overlapping external influence factors (e.g. loess thickness, landscape position, surface and subsurface flow, impermeable base layers, etc.).

Reply: Thank you for your suggestion. We have added the following discussion.

We should be aware that the formation of soil pipes and sinkholes is not determined by a single factor, but rather results from the interplay of interconnected geomorphic processes and overlapping external influence factors (e.g., loess thickness, landscape position, surface and subsurface flow, impermeable base layers, etc.). Conversely, the

development of soil pipes and sinkholes can further undermine slope stability, intensify gully erosion, and induce geological hazards such as collapses, landslides, and debris flows.

l 774: The conclusion section refers to "hazard curves incorporating the time dimension (ie., timing of sinkhole occurrence)". However, this doesn't seem to be subject of the manuscript presented.

Reply: I completely agree with your comment. This sentence has now been removed.

 # Technical corrections

l 135: Clear object missing in "will make available"

Reply: We made the following changes: This will make available a unique case-study dataset to the global soil-piping community and will provide a scientific basis for assessing and managing sinkhole risk in the region.

l 193: Figure 2b caption: The 3D view behind the QR Code is very helpful. Consider adding the URL directly to the figure captions. Also consider english translations.

Reply: We have added the access URL (https://www.720yun.com/t/0cvktq7yg2w) for the UAV panoramic image in the figure caption, and labeled the content in both Chinese and English.

l 193: Figure 2c legend: "Qingshuiying group (Paleogene/EOGENE)" seems to be a typo, please use ICS terminology. Do you mean the 'N'eogene (system) or Eo'c'ene (series)?

Reply: Sorry, there was indeed a spelling error in the original figure legend. After checking the latest version of the International Chronostratigraphic Chart, the correct spelling should be Qingshuiying Group (Eocene-Oligocene).

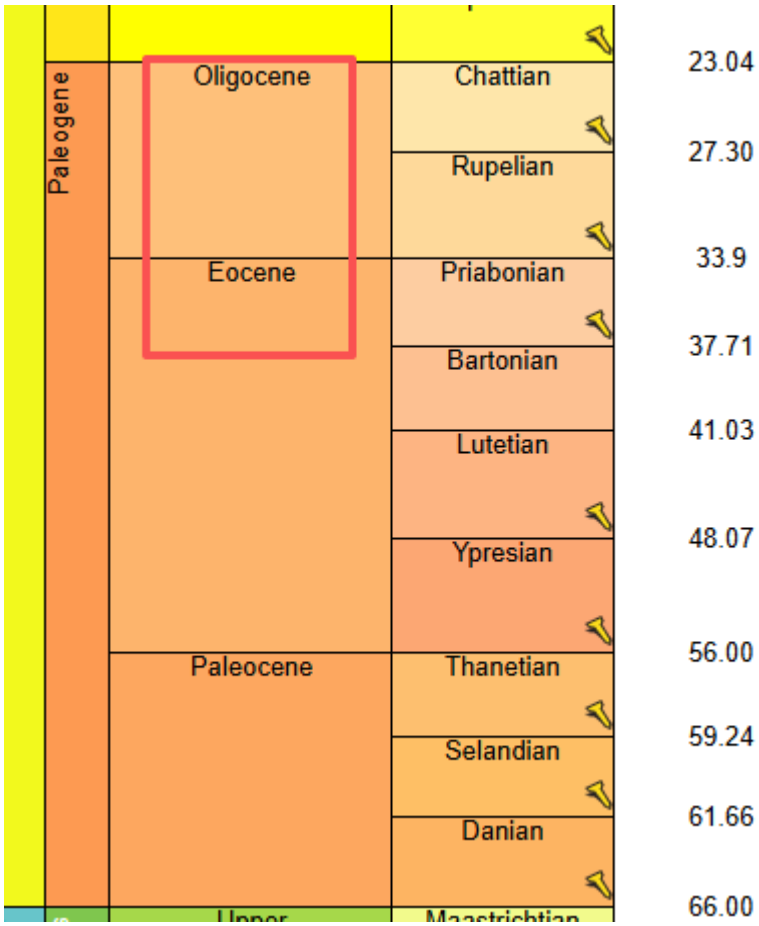

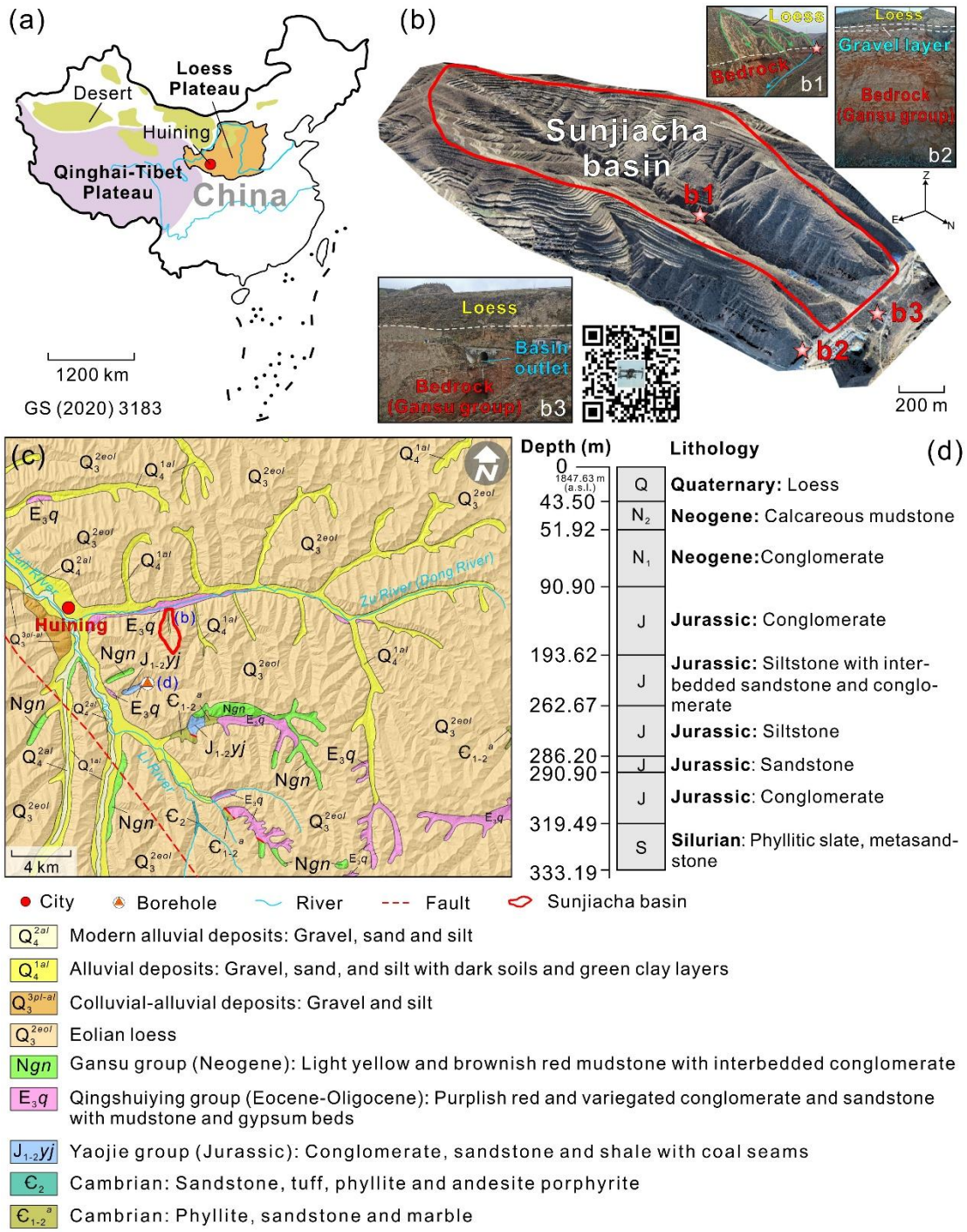

l 193: Figure 2d: Lithology "Neocene" -> Neogene

Reply: Have revised.

l 213f: Add software version numbers

Reply: Pix4D Mapper v4.5.6

l 222: Figure 4 says "Artificial extraction of sinkhole polygons". Did you mean

"Manual", as stated in l 215?

Reply: Yes, I have already revised Figure 4.

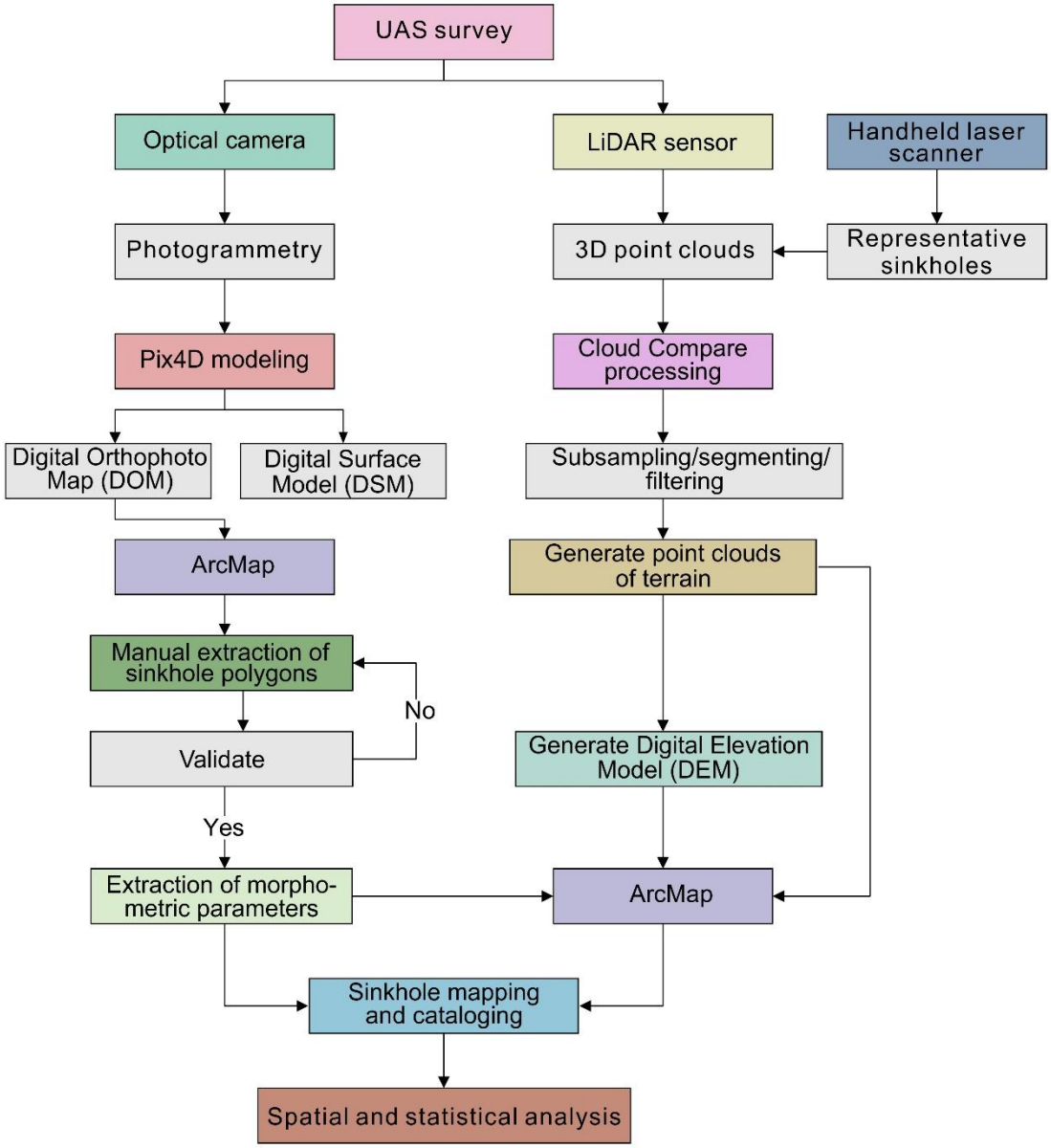

l 229: Which lidar detection mode (linear, geiger, etc.) does this scanner provide? URL is inconclusive.

Reply: The lidar detection mode of the D-LiDAR 2000 LiDAR sensor is linear scanning. I made annotations in the text: ……utilizing the D-Lidar 2000 LiDAR sensor (linear scanning)……

l 237: Add version number

Reply: UAV Manager v1.7.0

l 262: Add version number

Reply: GeoSLAM Draw v4.0 and Cloud Compare software v2.13.2

l 267: "Slop" -> slope

Reply: Have revised.

l 293: delete "some"

Reply: Have revised.

l 359ff: The absolute and relative numbers add up to 545+216+28=809 instead of 1194 sinkholes in total. Where's the rest?

Reply: Thank you very much for your careful observation! Let me explain why the total sample count of elevation is 809 rather than 1194: First, we indeed interpreted 1194 sinkholes from the UAV imagery, as the high-resolution images do allow us to identify smaller features (such as those with diameters less than 1 m). However, since the UAV flight altitude was around 200 m, the point cloud density from the airborne LiDAR was not particularly high. Our inspection revealed that the LiDAR point clouds were very sparse when detecting sinkholes with diameters below 1 m, with some sinkholes having only a few points, making it difficult to accurately capture parameters related to depth and volume. Therefore, when calculating maximum elevation, maximum depth, volume, and length to depth ratio, we only included sinkholes with diameters greater than 1 m. In fact, we have already indicated the sample sizes in Figure 9. To avoid any confusion, we feel it is necessary to provide a brief explanation in the main text of Section 4.3 Morphometric analysis. Thank you once again for your thoughtful comment!

4.3 Morphometric analysis

Here below we analyze the spatial and morphometric parameters computed for the 1194 inventoried sinkholes (1162 single, 32 compound), their frequency-size distribution

(Fig. 9), as well as some spatial patterns based on the distribution of different value ranges (Fig. 10). It should be noted that the airborne LiDAR returned sparse and limited point clouds when detecting sinkholes with diameters less than 1 m. When calculating parameters related to sinkhole depth and volume (e.g., Maximum Elevation, Maximum Depth, Volume, and Length-to-Depth Ratio), we retained only 809 sinkholes with diameters $\geqslant$1 m.

G	H	I	J	K	L	M	N	O	P	Q	R	S	T	U
方位角1	方位角2	最大高程	最小高程	平均高程	最大深度	周长	面积	体积	延伸率	直径/深度比	紧实度指数	圆度指数	土壤干密度	土壤流失量
Azimuth 1	Azimuth 2	Maximum elevation	Minimum elevati	Average elevatio	Maximum depth	Perimeter	Area	Volume	Elongation ratio	Length to Depth ratio	Compactness index	Circularity index	Soil dry density	Soil loss
Azi_1	Azi_2	Emax	Emin	Eave	Dmax	P	A	V	ER	LDr	COI	CLI	ρ_dry	SL
°	°	m	m	m	m	m	m^2	m^3	-	-	-	-	t/m^3	t
177.9	357.9	2016.66	2012.52	2014.50	4.14	14.52	15.44	63.89	1.48	1.28	0.81	0.92	1.274	81.39
10.0	190.0					2.74	0.57		1.17		0.77	0.95	1.274	
127.9	307.9					1.95	0.27		1.36		0.69	0.89	1.274	
24.6	204.6					2.58	0.40		1.36		0.69	0.76	1.274	
108.4	288.4	1987.40	1979.14	1984.46	8.26	15.61	18.78	155.15	1.11	0.63	0.76	0.97	1.274	197.66
21.8	201.8	1986.14	1979.61	1983.79	6.53	16.25	18.99	124.06	1.12	0.77	0.85	0.90	1.274	158.05
92.9	272.9	1985.51	1979.75	1982.47	5.76	18.79	26.00	149.68	1.38	1.18	0.77	0.93	1.274	190.70
41.6	221.6	1994.71	1991.88	1993.31	2.83	4.34	1.23	3.47	1.76	0.57	0.82	0.82	1.274	4.42
96.6	276.6	1995.06	1987.58	1992.65	7.48	6.42	3.15	23.54	1.05	0.27	0.80	0.96	1.274	29.99
125.4	305.4	2014.31	2009.89	2012.53	4.42	5.79	2.42	10.70	1.44	0.48	0.78	0.91	1.274	13.64
165.5	345.5	2013.60	2008.16	2011.10	5.44	7.04	3.61	19.62	1.14	0.42	0.80	0.91	1.274	25.00
114.4	294.4					2.80	0.58		1.40		0.79	0.93	1.274	
94.5	274.5					2.62	0.51		1.26		0.73	0.93	1.274	
137.8	317.8					2.36	0.39		1.47		0.76	0.87	1.274	
19.7	199.7					3.57	0.85		1.54		0.76	0.83	1.274	
76.9	256.9	1992.94	1991.58	1992.01	1.37	6.62	2.87	3.91	1.62	1.84	0.73	0.82	1.274	4.99
50.6	230.6	1992.82	1991.96	1992.33	0.85	4.00	1.18	1.01	1.40	1.68	0.81	0.93	1.274	1.28
149.5	329.5	1920.51	1919.01	1920.21	1.50	4.01	1.07	1.62	1.86	1.06	0.78	0.84	1.274	2.06
161.1	341.1	1920.52	1919.18	1920.17	1.34	4.00	1.10	1.47	1.63	1.14	0.77	0.86	1.274	1.88
19.2	199.2	1922.84	1918.25	1919.64	4.58	8.24	5.03	23.07	1.37	0.65	0.78	0.93	1.274	29.39
17.0	197.0	1958.50	1956.42	1957.73	2.09	10.39	3.64	7.60	1.95	1.84	0.48	0.42	1.274	9.68
42.7	222.7	1907.81	1904.86	1907.03	2.95	4.30	1.25	3.68	1.60	0.56	0.73	0.85	1.274	4.69
3.0	183.0					3.23	0.78		1.34		0.83	0.93	1.274	
159.4	339.4	1909.05	1907.21	1908.11	1.84	7.73	4.22	7.75	1.20	1.38	0.79	0.89	1.274	9.87
11.6	191.6					3.40	0.71		1.74		0.71	0.77	1.274	
2.3	182.3	1908.82	1908.24	1908.57	0.58	4.68	1.08	0.63	1.53	2.66	0.70	0.62	1.274	0.80
42.9	222.9	1908.93	1907.99	1908.44	0.94	9.94	5.97	5.63	1.36	3.70	0.67	0.76	1.274	7.17
8.3	188.3	1908.91	1906.97	1908.20	1.93	6.86	2.73	5.27	2.19	1.45	0.76	0.73	1.274	6.71
63.7	243.7	1862.44	1844.33	1852.14	18.11	57.75	236.27	4278.30	1.19	1.06	0.76	0.89	1.274	5450.55

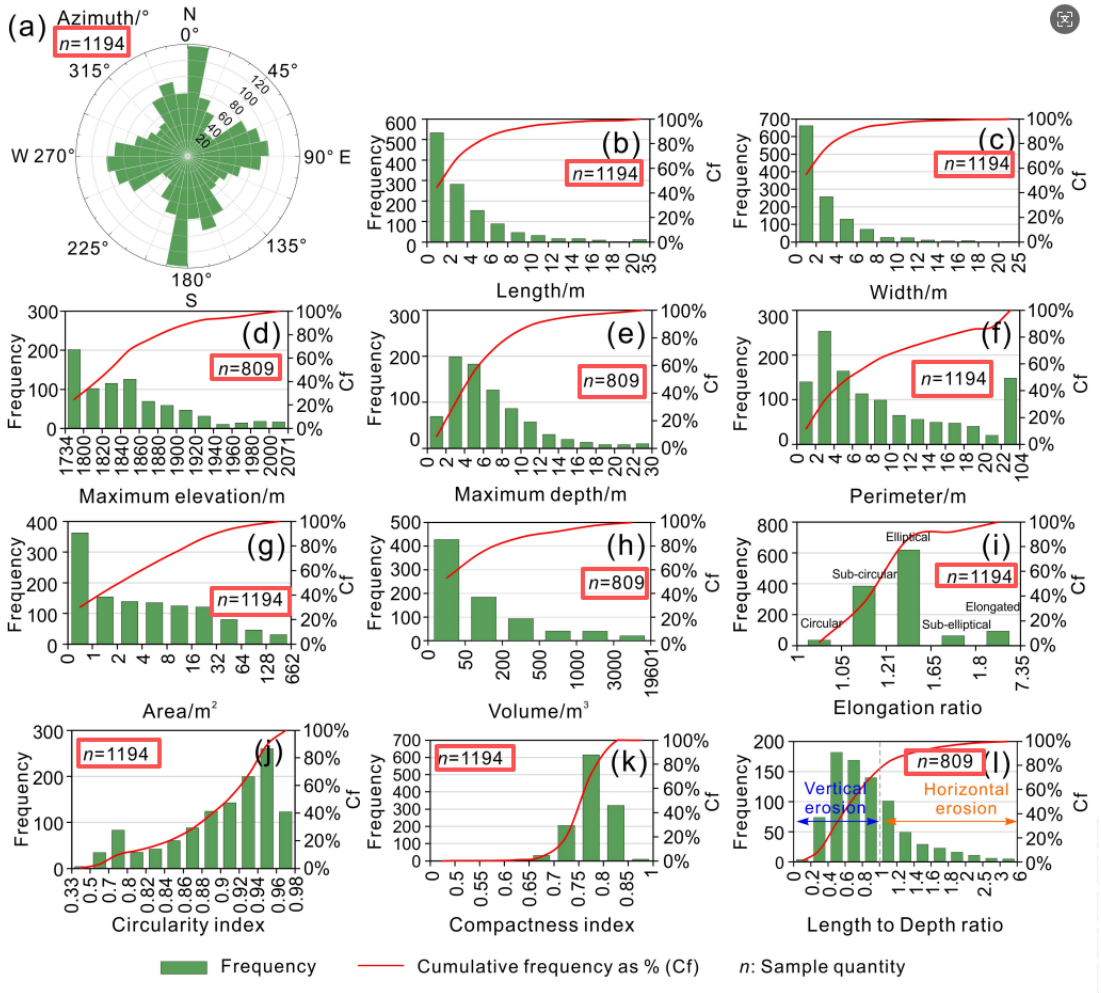

l 338: "un" -> in

Reply: I guess what you meant was line 388. I have made the correction.

l 402: cartographic -> spatial

Reply: Have revised.

l 410f: The relative numbers don't add up to 1194. 382/1194 is 32% (not 47%); 58/1194 is 5% (not 7%).

Reply: Thank you very much for your careful observation! Let me explain why the total sample count of elevation is 809 rather than 1194: First, we indeed interpreted 1194 sinkholes from the UAV imagery, as the high-resolution images do allow us to identify smaller features (such as those with diameters less than 1 m). However, since the UAV flight altitude was around 200 m, the point cloud density from the airborne

LiDAR was not particularly high. Our inspection revealed that the LiDAR point clouds were very sparse when detecting sinkholes with diameters below 1 m, with some sinkholes having only a few points, making it difficult to accurately capture parameters related to depth and volume. Therefore, when calculating maximum elevation, maximum depth, volume, and length to depth ratio, we only included sinkholes with diameters greater than 1 m. In fact, we have already indicated the sample sizes in Figure 9. To avoid any confusion, we feel it is necessary to provide a brief explanation in the main text of Section 4.3 Morphometric analysis. Thank you once again for your thoughtful comment!

l 415: 428/1194 is 36% (not 53%)

Reply: See the reply to the previous comment.

l 424: 569/1194 is 48% (not 70%)

Reply: See the reply to the previous comment.

l 426: 240/1194 is 20% (not 30%)

Reply: See the reply to the previous comment.

l 541: "root systems, AND human activity"

Reply: Have revised.

l 729: delete duplicate hyphen

Reply: Have revised.

l 825: "Brlmo" -> Bruno

Reply: Thank you for catching that! I checked the original manuscript and found that the author information in the Web of Science database was incorrect. We have corrected this error.

Bruno, E., Calcaterra, D., and Parise, M.: Development and morphometry of sinkholes in coastal plains of Apulia, southern Italy. Preliminary sinkhole susceptibility

assessment, Eng Geol, 99, 198–209, 10.1016/j.enggeo.2007.11.017, 2008.

Development and morphometry of sinkholes in coastal plains of Apulia, southern Italy. Preliminary sinkhole susceptibility assessment

By
Are you this author?

Brlmo, E (Brlmo, E.) [1] ; Calcaterra, D (Calcaterra, D.) [1] ; Parise, M (Parise, M.) [2]

View Web of Science ResearcherID and ORCID (provided by Clarivate)

Source ENGINEERING GEOLOGY

View Journal Impact

Volume: 99 Issue: 3-4 Page: 198-209
DOI: 10.1016/j.enggeo.2007.11.017

Published JUN 23 2008

Indexed 2008-06-23

Document Type Article; Proceedings Paper

Conference
Meeting: 1st General Meeting of the European-Geosciences-Union
Location: Nice, FRANCE
Date: APR 25-30, 2004
Sponsor: European Geosci Union

View PDF Download full issue

ELSEVIER

Engineering Geology
Volume 99, Issues 3–4, 23 June 2008, Pages 198-209

Development and morphometry of sinkholes in coastal plains of Apulia, southern Italy. Preliminary sinkhole susceptibility assessment

E. Bruno [a], D. Calcaterra [a], M. Parise [b]

Show more

+ Add to Mendeley Share Cite

https://doi.org/10.1016/j.enggeo.2007.11.017

Get rights and content

Full text access